PERGAMON

International Journal of Solids and Structures 36 (1999) 3339–3348

INTERNATIONAL JOURNAL OF SOLIDS and STRUCTURES

Mixed mode fracture in epicycloid specimens III. Dislocations

W. H. Müller[a,*], W. Littmann[b], H. Gao[c]

[a] *Department of Mechanical and Chemical Engineering, Heriot-Watt University, Edinburgh EH14 4AS, U.K.*
[b] *Heinz Nixdorf Institut, Mechatronik und Dynamik, Universität-Gesamthochschule-Paderborn, Fürstenallee 11, 33102 Paderborn, Germany*
[c] *Division of Mechanics and Computation, Durand Building, Stanford University, Stanford, CA 94305, U.S.A.*

Received 20 September 1997

Abstract

Complex stress potentials are derived to obtain an analytical solution for the stresses in epicycloidal specimens which contain a dislocation. The solution is used to obtain an analytical expression for the stress intensity factors of cusp-like cracks in such specimens which can be considered as a generalization of the well established concept of Griffith cracks. It is shown that by suitable positioning of the dislocation, both positive and negative mode I stress intensity factors will result. This illustrates the potential of epicycloid specimens for determination of fracture properties under compressive loading where frictional contact of the crack surfaces is a priori avoided.

1. On the use of epicycloid specimens in fracture mechanics

In two recent papers by Gao et al. (1998) and Müller and Gao (1998) the potential of epicycloid specimens for experimental determination of interface fracture properties as well as testing under compressive loading conditions has been explored. It was demonstrated that epicycloid specimens contain defects in the form of cusps which can be considered as a generalization of the traditional concept of a Griffith crack. So far the effects of thermo-mechanical loads (induced by a 'hot spot' region) and point forces have been explored. In this brief note the concept of epicycloid fracture specimens will be extended to include loading of epicycloid specimens by dislocations.

Recall that the generic mapping equation of the cycloid family is given by (cf. Bronstein and Semendjajew, 1976; Muskhelishvili, 1963):

* Corresponding author. Fax: 0131 451 3129; e-mail: w.h.muller@hw.ac.uk

0020–7683/99/$ - see front matter
PII: S0020–7683(98)00146–2

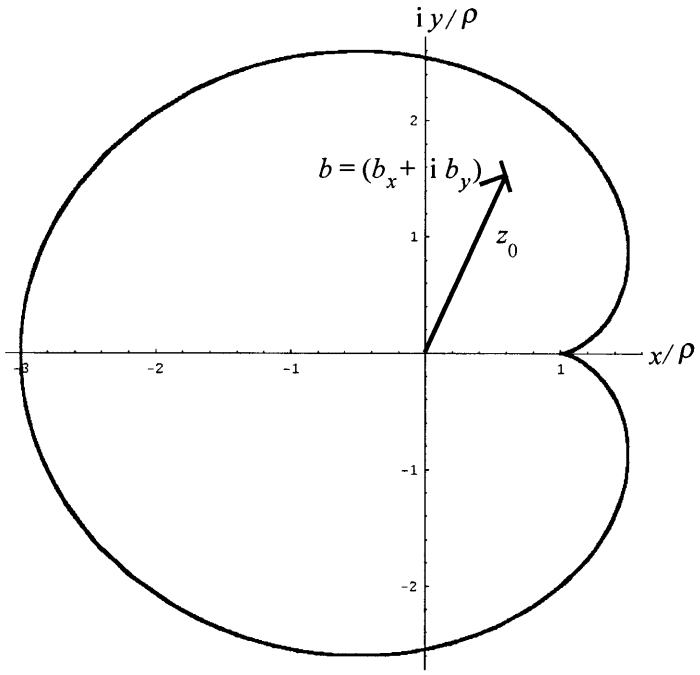

Fig. 1. An epicycloid specimen with a dislocation.

$$z = \omega(\zeta) = R\left(\zeta - \frac{\varepsilon}{n+1}\zeta^{n+1}\right), \quad \zeta = \exp(\mathrm{i}\vartheta), \quad R = (n+1)\rho \tag{1.1}$$

where $z = x + \mathrm{i}y$ is the position in the original complex plane $n \in \mathbb{N}$, $\vartheta \in [0, 2\pi)$, $\varepsilon \in [0, 1]$, and ρ is the radius of the revolving circle. Note that by putting $\varepsilon = 1$ epicycloids show the characteristic feature of cusp-like cracks. This is illustrated in Fig. 1 which shows an epicycloid with only one cusp, the case where $n = 1$. This contour is also known as Pascal's limaçon. As indicated in the figure the specimen contains a dislocation of strength $b = b_x + \mathrm{i}b_y$ (the Burgers vector) at the position z_0. It is well known that the presence of dislocations within a solid leads to the formation of stresses which in the present case give rise to a non-vanishing mixed-mode stress intensity at the crack tip.

The following analysis of the stresses and of the stress intensity factors focuses on the geometry shown in Fig. 1. However, an attempt is made to present the analysis such that, in principle, it can be generalized to cover other cases for which $n > 1$. It is worth mentioning that epicycloid specimens with cusp-like cracks can be treated analytically. In other words: epicycloids belong to the few fracture mechanics specimens of finite size which do not require numerical treatment such as boundary collocation or finite elements (cf. Tada et al., 1985). This was demonstrated in the aforementioned papers by the authors on this subject and it will now be shown that it also holds for loading by dislocations.

2. Stress analysis

2.1. Essentials of complex stress analysis

According to the concepts of two-dimensional theory of elasticity in complex variable notation the resultant force, F, acting on a line, L, can be obtained from:

$$F(z) = -\mathrm{i}[\varphi(\tilde{z}) + \tilde{z}\overline{\varphi'(\tilde{z})} + \overline{\psi(\tilde{z})}]_{\tilde{z}=a}^{\tilde{z}=z}, \quad \forall z \in L \tag{2.1}$$

where $[\,]_{\tilde{z}=a}^{\tilde{z}=z}$ denotes the increase undergone by the expression in brackets as the point $\tilde{z}$ passes along the line L from points a to z. The symbols $\varphi(z)$ and $\psi(z)$ denote the complex stress potentials of the Muskhelishvili–Kolosov equations (e.g., Sokolnikoff, 1956; Muskhelishvili, 1963):

$$\begin{aligned} \sigma_{yy} + \sigma_{xx} &= 2[\varphi'(z) + \overline{\varphi'(z)}], \\ \sigma_{yy} - \sigma_{xx} + 2\mathrm{i}\sigma_{xy} &= 2[\bar{z}\varphi''(z) + \psi'(z)]. \end{aligned} \tag{2.2}$$

and σ_{ij}, $i, j \in \{x, y\}$ are the stresses in rectangular coordinates. The periphery of the epicycloid specimen shown in Fig. 1 is supposed to be free of tractions and, therefore, it is necessary and sufficient that the resultant force, F, vanishes in each and every point, z, of it:

$$\varphi(z) + z\overline{\varphi'(z)} + \overline{\psi(z)} = 0, \quad \forall z \in L. \tag{2.3}$$

2.2. The stress potentials

According to the procedure presented in the papers by Gao et al. (1998) and Müller and Gao (1998) the stress potentials, $\varphi(z)$ and $\psi(z)$, are divided into two parts:

$$\varphi(z) = \varphi_\infty(z) + \varphi_s(z), \quad \psi(z) = \psi_\infty(z) + \psi_s(z). \tag{2.4}$$

The first part, identified by the index '∞', refers to the complex potentials that characterize the stresses at point z produced by a dislocation of strength $b_x + \mathrm{i}b_y$ at a position z_0 in an infinite plane (cf. Rice, 1968, pp. 226)[1]:

$$\varphi_\infty(z) = -\mathrm{i}A(b_x + \mathrm{i}b_y)\ln(z - z_0), \quad A = \frac{\mu}{\pi(\kappa+1)}, \quad \kappa = \begin{cases} 3-4\nu, & \text{plane strain} \\ \dfrac{3-\nu}{1+\nu}, & \text{plane stress} \end{cases}, \tag{2.5}$$

and:

$$\psi_\infty(z) = \mathrm{i}A(b_x - \mathrm{i}b_y)\ln(z - z_0) + \mathrm{i}A(b_x + \mathrm{i}b_y)\frac{\bar{z}_0}{z - z_0} \tag{2.6}$$

where μ denotes the shear modulus.

[1] Note that in Rice's article the dislocation is situated at a position, t, on the real axis. The stress potentials shown in eqns (2.5) and (2.6) follow by application of the transformation rules for complex potentials to the case of a dislocation positioned in the origin (see, e.g., Milne-Thomson, 1968, Section 2.21).

The second set of functions in eqn (2.4), identified by the subscript 's', must be chosen such that eqn (2.3) is satisfied, i.e.:

$$\varphi_s(z)+z\overline{\varphi_s'(z)}+\overline{\psi_s(z)} = -\varphi_\infty(z)-z\overline{\varphi_\infty'(z)}-\overline{\psi_\infty(z)}, \quad \forall z\in L. \tag{2.7}$$

It is useful to evaluate this condition on the unit circle. To this end the conformal mapping shown in eqn (1.1) is used which reads, in complex notation, for $n=1$, $\varepsilon=1$:

$$z=\frac{R}{2}\zeta(2-\zeta). \tag{2.8}$$

Moreover, since the potentials φ_s and ψ_s are analytical within the unit circle they can be represented by power series as follows:

$$\varphi_s(\zeta)=\sum_{m=1}^{\infty} a_m\zeta^m, \quad \psi_s=\sum_{m=1}^{\infty} b_m\zeta^m, \tag{2.9}$$

where rigid body displacements were ignored. Now the Cauchy operator:

$$\frac{1}{2\pi\mathrm{i}}\oint_{|\zeta|=1}\frac{(\cdot)\,\mathrm{d}\zeta}{\zeta-\eta}, \quad \forall|\eta|\leqslant 1 \tag{2.10}$$

is applied to the left hand side (LHS) of eqn (2.7) resulting in[2]:

$$\begin{aligned}\frac{1}{2\pi\mathrm{i}}\oint_{|\zeta|=1}\frac{\mathrm{LHS}\,\mathrm{d}\zeta}{\zeta-\eta} &= \sum_{m=1}^{\infty} a_m\eta^m+\frac{1}{2}\bar{a}_1\eta-\frac{1}{2}(\bar{a}_1\eta^2+2\bar{a}_2\eta)\\ &\equiv \varphi_s(\eta)+\frac{1}{2}\bar{a}_1\eta-\frac{1}{2}(\bar{a}_1\eta^2+2\bar{a}_2\eta).\end{aligned} \tag{2.11}$$

In order to determine the coefficients a_1 and a_2 the Cauchy operator of eqn (2.10) is also applied to the various terms shown on the right hand side (RHS) of eqn (2.7). By means of Cauchy's theorem it can be shown that:

$$\begin{aligned}&-\frac{1}{2\pi\mathrm{i}}\oint_{|\zeta|=1}\frac{(\varphi_\infty(\zeta)+z\overline{\varphi_\infty'(z)}+\overline{\psi_\infty(z)})\,\mathrm{d}\zeta}{\zeta-\eta}\\ &\qquad = \mathrm{i}A\left((b_x+\mathrm{i}b_y)[\ln(1-\eta\overline{\zeta_0})+\ln(2-\eta-\zeta_0)]-(b_x-\mathrm{i}b_y)\oint_{|\zeta|=1}\frac{G(\zeta,\zeta_0)\,\mathrm{d}\zeta}{\zeta-\eta}\right)\end{aligned} \tag{2.12}$$

with the following contraction:

[2] See Gao et al. (1998) for further details of the proof for arbitrary values of n and ε.

$$G(x,t)=\frac{(x-t)(2-x-t)}{\left(\frac{1}{x}-\bar{t}\right)\left(2-\frac{1}{x}-\bar{t}\right)} \tag{2.13}$$

and constant terms have been omitted.

The symbol ζ_0 allows one to identify the position of the dislocation in the plane of the unit circle and is related to the location z_0 in the original plane as follows [cf. eqn (2.8)]:

$$z_0=\frac{R}{2}\zeta_0(2-\zeta_0)\Rightarrow z-z_0=\frac{R}{2}(\zeta-\zeta_0)(2-\zeta-\zeta_0). \tag{2.14}$$

The remaining Cauchy integral in eqn (2.12) was solved by application of the residue theorem using Mathematica®. Because the result is lengthy it will not be repeated here in detail. In the next step eqn (2.12) was expanded in terms of the variable η. This allows one to identify the coefficients λ_1 and λ_2 in the following series:

$$\frac{1}{2\pi\mathrm{i}}\oint_{|\zeta|=1}\frac{\mathrm{RHS}\,\mathrm{d}\zeta}{\zeta-\eta}=\sum_{i=1}^{\infty}\lambda_i\eta^i. \tag{2.15}$$

The explicit mathematical form of these coefficients is quite unwieldy and will not explicitly be presented in this paper. By comparison of eqn (2.19) with eqn (2.14) the following relations for the unknown coefficients a_1 and a_2 are obtained:

$$a_1+\tfrac{1}{2}\bar{a}_1-\bar{a}_2=\lambda_1,\quad a_2-\tfrac{1}{2}\bar{a}_1=\lambda_2 \tag{2.16}$$

from which the real parts can be determined:

$$\mathrm{Re}\,a_1=\lambda_1+\overline{\lambda_2},\quad \mathrm{Re}\,a_2=\tfrac{1}{2}(\lambda_1+\lambda_2+2\overline{\lambda_2}). \tag{2.17}$$

In fact, it is sufficient to determine the real parts of these coefficients since their imaginary parts contribute only to a rigid body rotation which will be suppressed (see Müller and Gao, 1998, for the proof).

By combination of eqns (2.4)–(2.6), (2.12) it finally follows for the complex potential $\varphi(\eta)$:

$$\varphi(\eta)=\mathrm{i}A(b_x+\mathrm{i}b_y)\ln\frac{1-\eta\overline{\zeta_0}}{\eta-\zeta_0}-\mathrm{i}A(b_x-\mathrm{i}b_y)\oint_{|\zeta|=1}\frac{G(\zeta,\zeta_0)\,\mathrm{d}\zeta}{\zeta-\eta}-\left[\frac{1}{2}\bar{a}_1\eta-\frac{1}{2}(\bar{a}_1\eta^2+2\bar{a}_2\eta)\right]. \tag{2.18}$$

The second potential $\psi(\eta)$ can directly be obtained from eqn (2.7) as described in Gao et al. (1998).

2.3. Stress intensity factors for the cusp in a Pascal's limaçon specimen

The stress intensity factors (SIFs), K_{I} and K_{II}, of a cusp in an epicycloid can be determined from the following equation (see Gao et al., 1998):

$$K_{\mathrm{I}} - \mathrm{i}K_{\mathrm{II}} = -\lim_{z_c \to 0} \{2\sqrt{-2\pi z_c}\varphi'(z_c)\} \tag{2.19}$$

where z_c denotes a complex vector originating at the tip of the cusp. Performing the limit yields for an epicycloid specimen of the Pascal's limaçon type:

$$K_{\mathrm{I}} - \mathrm{i}K_{\mathrm{II}} = 2\sqrt{\frac{\pi}{R}}\varphi'(\zeta = 1). \tag{2.20}$$

The explicit formula for the SIFs for arbitrary positioning of the dislocation, i.e., arbitrary value of ζ_0, is comparatively long and, therefore, will be omitted in this paper. In the following section the qualitative behavior of the SIFs will be discussed and explicit expressions for the SIFs will be presented for the case of a dislocation positioned along the real axis.

3. Results and discussion

The sequence in Fig. 2 allows one to gain an overview of the SIFs obtained from numerical evaluation of eqns (2.18) and (2.20) for the cases $b_x = 0$, $b_y = 1$ or $b_x = 1$, $b_y = 0$ for all possible locations $z_0 = x_0 + \mathrm{i}y_0$ of the dislocation (cf. Fig. 1). The SIFs were normalized by:

$$K_0 = A\sqrt{\frac{2}{R}}. \tag{3.1}$$

The following features of the solution are clearly discernible:

- The SIFs become singular if the dislocation is moved toward the tip of the cusp.
- Within the epicycloid there are large regions of alternating K_{I} and K_{II}-sign.
- In the case $b_x = 0$, $b_y \neq 0$, K_{I} is symmetric and K_{II} is anti-symmetric with respect to the symmetry axis of the epicycloid. The opposite is true in the case $b_x \neq 0$, $b_y = 0$.
- The dislocations can be positioned such that pure mode I and mode II conditions result.

These statements are more closely examined in the sequence of Fig. 3 which shows 'lines of blind spots' where either K_{I} and K_{II} are zero and which separate regions of different K-sign.

For example: if a dislocation of strength $b_x = 0$, $b_y \neq 0$ is positioned within the left region shown in Fig. 3(a) negative K_{I}-values result whereas a dislocation in the right hand side leads to a crack opening mode. Figure 4(a) allows one to understand this phenomenon in a more intuitive way. It shows a Volterra dislocation within the epicycloid the presence of which may lead to negative or positive 'bending moments', depending on the position.

On the other hand if a dislocation of strength $b_x \neq 0$, $b_y = 0$ is positioned in the upper half of the epicycloid shown in Fig. 1 this will result in a closing of the cusp whereas the same dislocation in the lower half gives rise to positive K_{I}-values: Fig. 3(b). This behavior is illustrated in Fig. 4(b).

By comparison of Figs 3(a) and (c) as well as Figs 3(b) and (d) it becomes possible to identify those points for which either pure mode I or pure mode II conditions exist.

Following Ravi-Chandar and Knauss (1984) the situations depicted in Fig. 4 could be realized experimentally by insertion of an insulated double-layered metal strip into the cut. If an electric current flows through this strip electromagnetic repulsion results which would separate the flanks

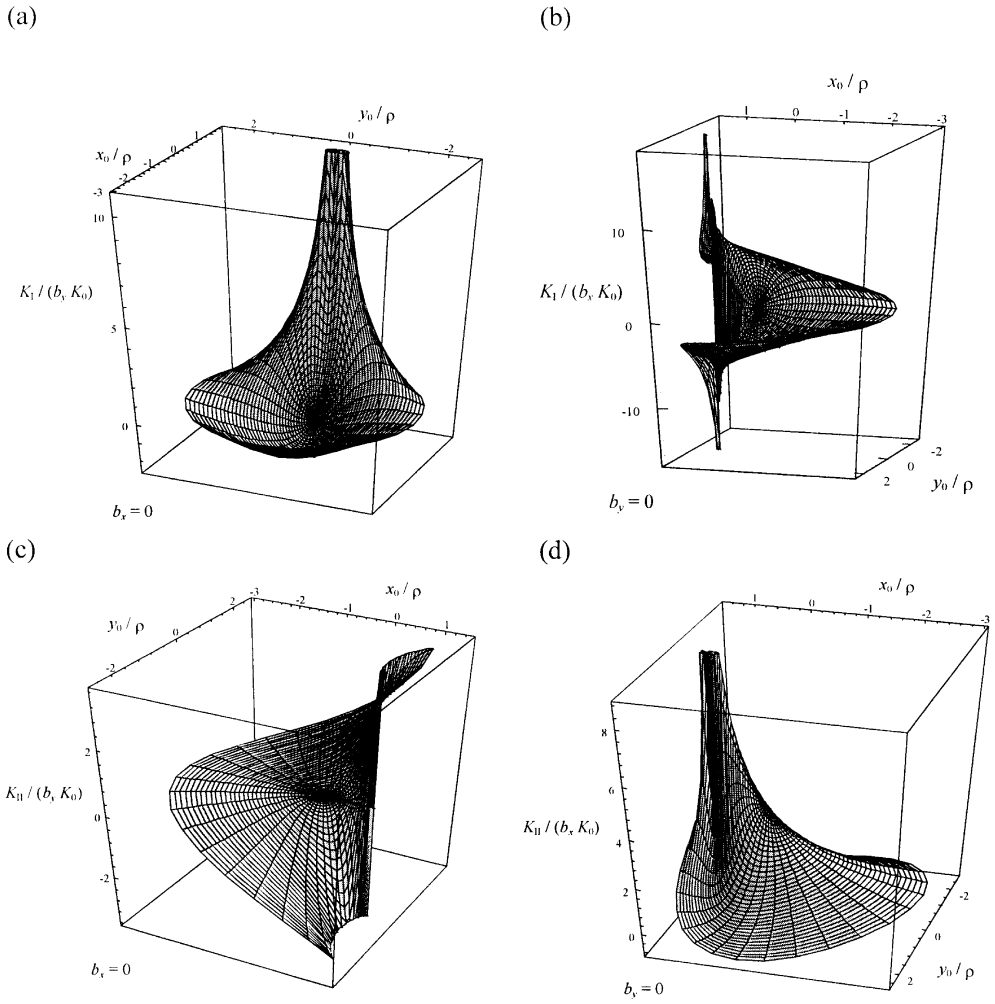

Fig. 2. Overview of SIFs for $b_x = 1$, $b_y = 0$ (b, d) and $b_x = 0$, $b_y = 1$ (a, c) for all possible positions z_0 within Pascal's limaçon.

of the cut and, consequently, simulate the opening induced by a dislocation. Depending on the toughness of the specimen and the intensity of the current it would also be possible to induce dynamic fracture in the epicycloid specimen. However, the analysis of the dynamic case would necessitate the derivation of dynamic SIFs.

The SIFs along the symmetry line, i.e., on the real axis $z_0 = x_0$, can be obtained from the following concise equations[3]:

[3] Which were obtained through symbolic evaluation of eqns (2.18) and (2.20) by means of Mathematica®.

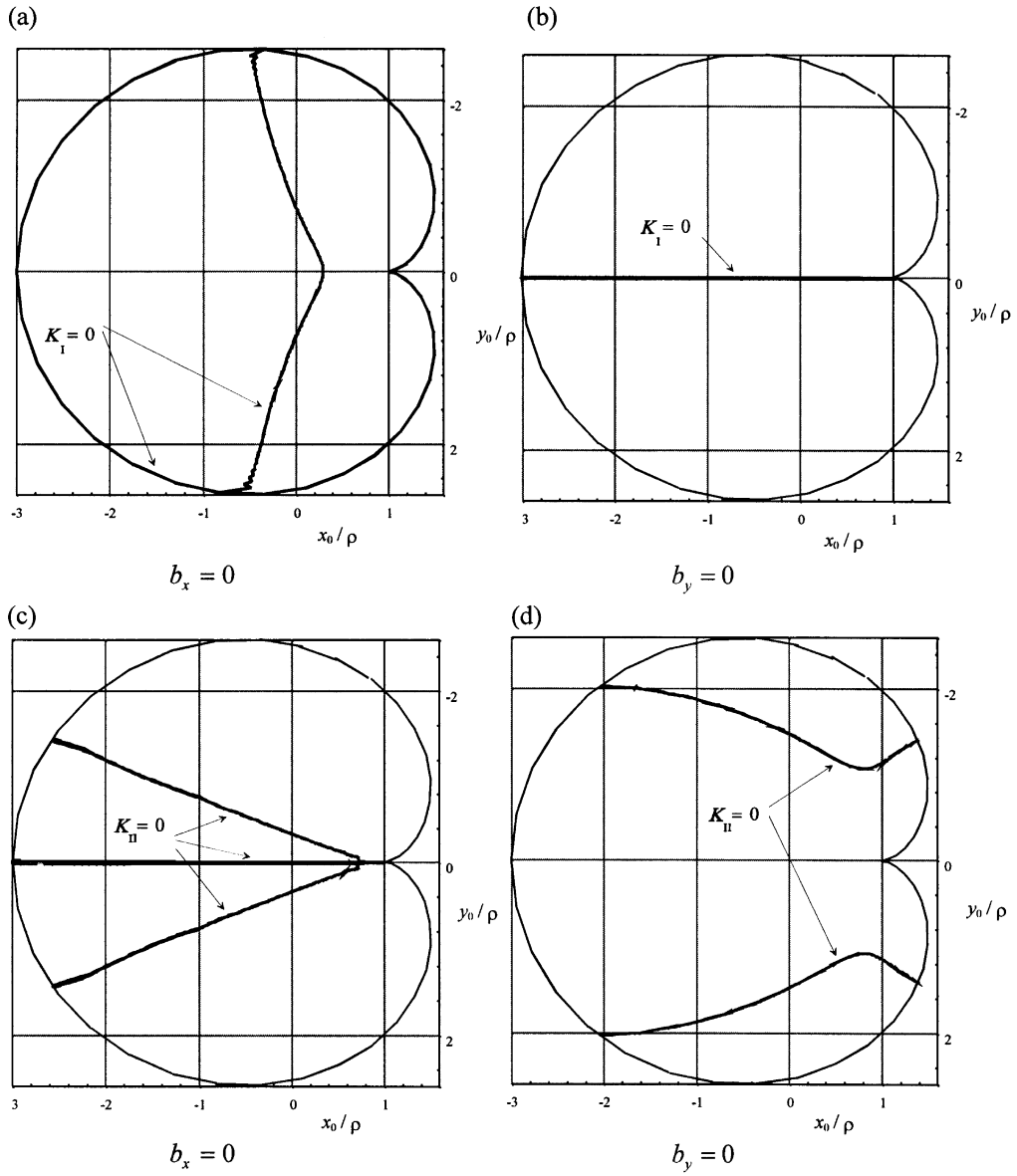

Fig. 3. Lines of blind spots for the four cases shown in Fig. 2.

$$\frac{K_{\mathrm{I}}}{K_0} = -b_y\sqrt{\frac{\pi}{2}}\frac{1-6\zeta_0-3\zeta_0^2+4\zeta_0^3}{1-\zeta_0},$$

$$\frac{K_{\mathrm{II}}}{K_0} = b_x\sqrt{\frac{\pi}{2}}\frac{11-4\zeta_0-5\zeta_0^2+2\zeta_0^3}{(2-\zeta_0)^2(1-\zeta_0)}, \quad \zeta_0 = 1-\sqrt{1-\frac{x_0}{\rho}}. \tag{3.2}$$

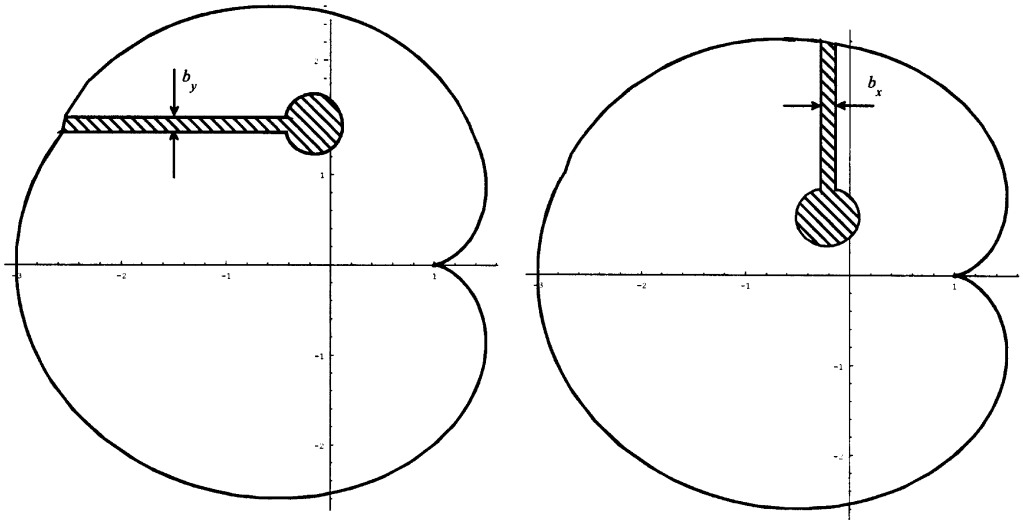

Fig. 4. A Volterra dislocation of the opening and of the shear type within the epicycloid.

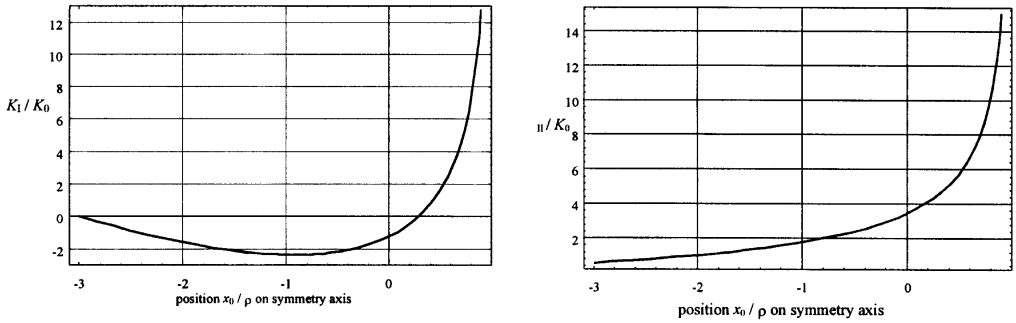

Fig. 5. Behavior of SIFs along the axis of symmetry of Pascal's limaçon.

Figure 5 shows a graphical representation of this result. As it was mentioned before the SIFs go to infinity if the dislocation moves closer toward the tip of the cusp and to zero if the dislocation is at the periphery $\zeta_0 = -1$. Especially noteworthy is the fact that positioning of the dislocation at most points of the symmetry line will lead to a negative K_I-value.

4. Conclusions

This paper draws attention to the potential of epicycloid specimens in fracture mechanics testing. To this end an analytical solution for the stresses in such specimens is derived, based on complex potential theory. Furthermore, the solution is specialized to the loading case of a dislocation within an epicycloid of the Pascal's limaçon type. The solution is used to derive analytical expressions for the mode I stress intensity factor of the cusp-like crack in that specimen. This solution is numerically

evaluated for various positions of the applied point forces. It is demonstrated by the calculated values that strongly negative K_I-conditions can be enforced without frictional contact and shear of the crack surfaces when the point forces take suitable positions.

Acknowledgements

The foundations to this paper were laid during a sabbatical visit of one of the authors (H.G.) to the Universität-Gesamthochschule-Paderborn at the beginning of 1996. The stay was financially supported by the Kommission für Forschung und wissenschaftlichen Nachwuchs der Universität Paderborn. This support is gratefully acknowledged. The authors would also like to thank the head of the Laboratorium für Technische Mechanik, o. Prof. Dr rer. nat. K. P. Herrmann, for his hospitality and support.

References

Bronstein, I.N., Semendjajew, K.A., 1976. Taschenbuch der Mathematik. 16. Auflage. Verlag Harri Deutsch, Zürich, Frankfurt/Main, Thun.

Gao, H., Müller, W.H., Kemmer, G., 1998. Mixed mode fracture in epicycloid specimens I. Thermal inclusions. Int. J. Solids Structures 35(14), 1617–1633.

Milne-Thomson, L.M., 1968. Plane Elastic Systems. Springer-Verlag, Berlin, Heidelberg, New York.

Müller, W.H., Gao, H., 1998. Mixed mode fracture in epicycloid specimens II. Point force loading. Int. J. Solids Structures 35(3–4), 205–217.

Muskhelishvili, N.I., 1963. Some Basic Problems of the Mathematical Theory of Elasticity, fourth, corrected and augmented edition. P. Noordhoff Ltd, Groningen-Netherlands.

Ravi-Chandar, K., Knauss, W.G., 1984. An experimental investigation into dynamic fracture I. Crack initiation and arrest. Int. J. Fract. 26, 65–80.

Rice, J.R., 1968. Chapter 3 Mathematical Analysis of the Mechanics of Fracture. In: Liebowitz, H. (Ed.), Fracture: An Advanced Treatise, Volume II Mathematical Fundamentals. Academic Press, New York, London.

Sokolnikoff, I.S., 1956. Mathematical Theory of Elasticity, 2nd ed. McGraw-Hill, New York, Toronto, London.

Tada, H., Paris, P.C., Irwin, G.R., 1985. The Stress Analysis of Cracks Handbook. Del Research Corporation, St Louis, Missouri.